East European Journal of Physics. **2.** 257-266 (2023)
DOI:10.26565/2312-4334-2023-2-29 ISSN 2312-4334

MAGNETO-THERMOELECTRIC COEFFICIENTS OF HEAVILY DOPED N-TYPE Mg_2Si MATERIAL[†]

Mulugeta Habte Gebru
Department of Physics, Arba Minch University, Arba Minch, Ethiopia
E-mail: mulugeta1970@gmail.com
Received March 27, 2023; revised April 26, 2023; accepted April 27, 2023

In contrast to parabolic band model typically used in understanding electronic properties in general, thermoelectric and magneto-thermoelectric in particular, this study confirms non-parabolic band model results in better understanding of Seebeck coefficient and Nernst coefficient in the presence of magnetic field for Mg_2Si. The magneto Seebeck coefficient was found significantly enhanced from its non-zero field value as a function of magnetic field for different electron concentrations in the range $0.6\text{-}12\times10^{25}/m^3$ on the average at room temperature for non-parabolic model compared to parabolic band model. The result for Nernst coefficient shows increasing trend as function of magnetic field except for certain electron concentrations for parabolic band model while it is decreasing with magnetic field on average for non-parabolic band model.
Keywords: *Magneto-Seebeck coefficient; Nernst coefficient; heavily doped semiconductor; magneto-thermoelectricity; magnesium Silicide*
PACS:72.20. My

INTRODUCTION

According to [1] Mg_2Si have been investigated both by experimental and theoretical approaches. By contrast, transport properties have never been determined so far using calculation methods so that the present study is among such few studies. The crystal structure data revealed that Mg_2Si has space group of Fm3m with Mg occupied sites in 8c (1/4,1/4,1/4) coordinates and Si occupied sites in 4a (0,0,0) coordinates [2].

In n-type Mg_2Si crystal doped with more than $6\times10^{16}/cm^3$ or more shallow donors concentration, the donor band merges with the conduction band [3]. The effect of heavily doping on electronic properties of semiconductors becomes important. There are a number of papers in literature [4,5] which show bit of data on electrical properties of heavily doped semiconductors. Recently, considerable interest has been aroused in the properties of heavily doped semiconductors because of their use in diodes and thin solar cells [6,7]. Heavily doped semiconductor based thermoelectric devices as a single device have been widely utilized as non-contact temperature sensors, flow sensors, gas sensors, accelerometers, and power generators while array of them as infrared (IR) imaging devices and micro-spectrometers [8]. It can be used for CNT application [9] and Lithium battery components [2].

Thermoelectric effects are in general dependent on magnetic field with the principal parameters, used in thermoelectric, the Seebeck and Peltier effects having the corresponding thermomagnetic coefficients the Nernst and Ettingshausen effects, respectively [12].

In [13] reported on the role of impurities on the lattice dynamics of nanocrystalline Si produced by a bottom-up process with respect to thermoelectric applications. [14] accounts the fact that when the doping density increases there are at least four phenomena occurring simultaneously, on one hand the conduction band and valence band rigidly shift towards one another due to increasing interactions among free carriers, and between free carriers and dopant atoms, causing a reduction in the band gap, in addition to this the two band edges are perturbed and band tails are formed, arising from the random impurity distribution and the resulting potential energy fluctuation.The next phenomena occurred is the shallow dopant band, located slightly above the valence band and the last one is Fermi level shift.

The review work by [15] discusses the nature of main factors such as impurities, defects, electrically active thermal donors and other complexes that are formed due to direct impurity scattering, acoustic phonon scattering, and optical phonon scattering etc. do influence the energy band structure formation in semiconductors, basic electrophysical, optical, thermoelectrical, even mechanical properties. [16] suggested the following expression for density of states of non-parabolic band having band tails

$$\rho(z) = \frac{m_b^{*\frac{3}{2}} 2^{\frac{3}{4}} \delta^{\frac{1}{2}}}{\pi^2 \hbar^3} y(z) \tag{1}$$

where,

$$y(x) = \frac{1}{\sqrt{\pi}} \int_{-\infty}^{z} \sqrt{z-\zeta}\, \exp(-\zeta^2) d\zeta \tag{2}$$

and

$$z = \frac{\varepsilon}{\sqrt{2}\delta} \tag{3}$$

[†] ***Cite as:*** M.H. Gebru, East Eur. J. Phys. **2**, 257 (2023), https://doi.org/10.26565/2312-4334-2023-2-29

For high density limit the potential energy fluctuation reduces to a Gaussian with the standard deviation of

$$\delta = \left(\frac{ne^4 a_s}{8\pi\epsilon_0^2\epsilon_d^2}\right)^{\frac{1}{2}} = \left(\frac{N_d e^4 a_s}{8\pi\epsilon_0^2\epsilon_d^2}\right)^{\frac{1}{2}} \tag{4}$$

We have a screened coulomb potential of impurity atoms with ϵ_d (dielectric constant) of the given semiconductor. The Thomas-Fermi screening length for all ionized dopants ($n \cong N_d$) according to [17] is

$$a_s = \left(\frac{\pi^{\frac{4}{3}}\epsilon_0\epsilon_d\hbar^2}{3^{\frac{1}{3}}N_d^{\frac{1}{3}}e^2 m_n^*}\right)^{\frac{1}{2}} \tag{5}$$

The density of states function given by equation (1) is very complicated and thus is not useful for making any calculation. Slotboom [18] has however; suggested the following approximation for y(z) as

$$\begin{cases} y(z) \cong z^{\frac{1}{2}}\left[1 - \frac{1}{16z^2}\right] \\ \quad ; \text{for } z > 0.601, equally, \varepsilon > 0.85\delta \\ y(z) \cong \frac{1}{2\pi^{\frac{1}{2}}} Exp(-z^2)\{1.225 - 0.906[1 - Exp(2z)]\} \\ \quad ; \text{for } z \leq 0.601 \end{cases} \tag{6}$$

We obtain the following expression of the electron concentration,

$$n = \frac{m_n^{*\frac{3}{2}} 2^{\frac{5}{4}} \delta^{\frac{3}{2}}}{\pi^2\hbar^3}\psi_0 \tag{7}$$

where,

$$\psi_0 = \frac{1}{2\pi^{\frac{1}{2}}}\int_{-\infty}^{0.601} \exp(-z^2)\left(\frac{0.319+0.906Exp(2z)}{1+Exp\left\{1.494n_n^{\frac{5}{12}}z-\eta\right\}}\right)dz + \int_{0.601}^{\infty} \frac{z^{\frac{1}{2}}\left[1-\frac{1}{16z^2}\right]}{1+\exp\left\{1.494n_n^{\frac{5}{12}}z-\eta\right\}}dz \tag{8}$$

The corresponding expressions for parabolic density of state and the electron concentration are

$$\rho(\varepsilon) = \frac{8\sqrt{2}\pi m_n^{*\frac{3}{2}}}{h^3}\varepsilon^{\frac{1}{2}} \tag{9}$$

and

$$n = \int_0^{\infty} \rho(\varepsilon) f_0(\varepsilon) d\varepsilon = \frac{m_n^{*3}}{2\pi^2\hbar^3}\left(\frac{2k_B T}{m_n^*}\right)^{\frac{3}{2}} F_{\frac{1}{2}}(\eta) \tag{10}$$

where, the standard Fermi-Dirac integral is

$$F_i(\eta) = \int_0^{\infty} \frac{x^i d\varepsilon}{(1+Exp[x-\eta)} \tag{11}$$

In terms of the reduced energy and Fermi energy $x = \frac{\varepsilon}{k_B T}$ and $= \frac{E_F}{k_B T}$, respectively. Thus, $F_{1/2}$ corresponds to i = ½.

It is more convenient to introduce normalized electron concentration n_n given by

$$n_n = \frac{n}{10^{25}/m^3}. \tag{12}$$

In this study the semi-classical and quantum treatments are applied in the calculations of scattering mechanisms under the assumptions of the electron concentrations from 0.6×10^{18} - $12\times10^{20}/cm^3$ and in the temperature range 77 – 300K.

BOLTZMANN TRANSPORT EQUATION WITH RELAXATION TIME APPROXIMATION

We define a probability density function f(**r**,**k**,t) that describes the probability of finding an electron at position **r** with a wave vector **k** at time t. The distribution function can be written as

$$f = f_0 + f_1 \tag{13}$$

where f_0 is the thermal equilibrium distribution and f_1 is a small perturbation.

The Boltzmann transport equation is

$$\frac{\partial f}{\partial t} + \mathbf{v}.\nabla \mathrm{f} + \dot{\mathbf{k}}.\nabla_{\mathrm{k}} \mathrm{f} = \left(\frac{\partial \mathrm{f}}{\partial \mathrm{t}}\right)_{\mathrm{C}} \tag{14}$$

Making use of $\mathrm{v} = \frac{1}{\hbar}\nabla_{\mathrm{k}}\varepsilon$ and $\nabla_k f_0 = \frac{\hbar^2 k}{m_n}\frac{df_0}{d\varepsilon}$ and assumption that $\nabla_r T$, $\nabla_r \varepsilon_F$ as well as the electric field E are first order quantities and on equating the first order terms in equation (14) to obtain

$$\frac{f_1}{\tau} = -\mathbf{v}.\left(\nabla_{\boldsymbol{r}}\varepsilon_f + \left(\varepsilon - \varepsilon_f\right)\nabla_{\boldsymbol{r}} T\right)\left(\frac{df_0}{d\varepsilon}\right) = -\mathbf{v}.\boldsymbol{F}.\left(\frac{df_0}{d\varepsilon}\right) \tag{15}$$

where,

$$\mathbf{F} = \nabla_{\boldsymbol{r}}\varepsilon_f + \left(\varepsilon - \varepsilon_f\right)\nabla_{\boldsymbol{r}} T \tag{16}$$

In the presence of Lorenz force consisting of magnetic field that created second order perturbation where f_1 is assumed to behave as a negative scalar function of the energy ε as

$$\mathrm{f}_1 = -\phi\frac{\mathrm{df}_0}{\mathrm{d}\varepsilon} \tag{17}$$

where,

$$\phi = \tau\mathbf{v}.\mathbf{G} \tag{18}$$

when **B** = 0 the general vector **G** reduces to **F** for electric field only.

We can say the collision process can be described such that the loss of momentum **P**/τ is described by the Lorenz equation

$$m_n^* \frac{d\mathbf{v}}{dt} = (-e)(\boldsymbol{E} + \mathbf{vxB}) - \frac{\mathbf{P}}{\tau} \tag{19}$$

Similarly,

$$\frac{\phi}{\tau} = \mathbf{v}.\left(\nabla_{\boldsymbol{r}}\varepsilon_F + \frac{\varepsilon - \varepsilon_F}{T}\nabla_{\mathbf{r}}\mathrm{T}\right) - (-e)(\mathbf{E} + \mathbf{vxB}) \tag{20}$$

For spherically symmetric $\varepsilon(k)$ with $\mathbf{n} = \frac{\mathbf{k}}{k} = \frac{\mathbf{v}}{\mathrm{v}}$, and making appropriate coordinate transformations

$$e(\mathbf{v}\mathrm{X}B)\nabla_k\phi = \frac{ev}{k}(\mathbf{B}\mathrm{X}\,\phi)\mathbf{n} \tag{21}$$

We can express Eq.(20) as

$$\frac{\phi}{\tau} = \mathbf{v}.\left(\nabla_{\boldsymbol{r}}\varepsilon_F + \frac{\varepsilon - \varepsilon_F}{T}\nabla_{\mathbf{r}}\mathrm{T}\right) - \frac{ev}{\hbar k}(\mathbf{B}\mathrm{X}\phi).\mathbf{v} \tag{22}$$

For the case of transverse magnetic field **B** perpendicular to the field $E = E_x$ and thermal gradient in the x-y plane, the components of ϕ are

$$\frac{\phi_x}{\tau} = \mathrm{v}_x\left(\frac{d\varepsilon_F}{dx} + \frac{\varepsilon - \varepsilon_F}{T}\frac{dT}{dx}\right) - \frac{e\mathrm{v}_x^2}{\hbar k}B\phi_y \tag{23}$$

$$\frac{\phi_y}{\tau} = \mathrm{v}_y\left(\frac{d\varepsilon_F}{dy} + \frac{\varepsilon - \varepsilon_F}{T}\frac{dT}{dy}\right) + \frac{e\mathrm{v}_y^2}{\hbar k}B\phi_x \tag{24}$$

Solving for ϕ_x and ϕ_y gives

$$\phi_{\mathrm{x,y}} = \left(\tau\mathrm{v}_{\mathrm{x,y}}^2\mathrm{F}_{\mathrm{x,y}} \mp \omega\tau^2\mathrm{v}_{\mathrm{x,y}}^2\mathrm{F}_{\mathrm{y.x}}\right)/(1 + \omega^2\tau^2) \tag{25}$$

Where $\omega = \frac{\mathrm{eB}}{\mathrm{m}_{\mathrm{n}}^*}$ is cyclotron frequency.

DERIVATION OF CONDUCTIVITY FOR PARABOLIC AND NON-PARABOLIC BAND STRUCTURES

In reality there is a dynamic equilibrium maintained between energy input in the form of both heat and the electromagnetic forces and the scattering processes which tend to randomize momentum and relax energies. In the derivation of conductivities, we have assumed that

(i) the electrons are behaving identically with a uniform velocity.

(ii) the ionized impurity scattering is the most important for the electronic transport processes in heavily doped semiconductor and it is energy dependent ($\tau = \tau_0\varepsilon^{3/2}$) since most phonon modes would be suppressed at low temperatures in the range 77-300K and τ_0 is approximated to be 0.01 ns [19].

f_1 is responsible for the electric current density and the calculation of the electric current density lies within the first Brillouin zone with $\rho(k) = 1/4\pi^3$ is the local density of states in k-space to get after some steps.

$$J_x = \int_0^\infty ev_x^2 \phi_x \left(\frac{df_0}{d\varepsilon}\right) \rho d\varepsilon$$

$$= \sigma_{xx}E_x - \sigma_{xy}E_y + \frac{1}{T}\frac{dT}{dx}\alpha_{xx} - \frac{1}{T}\frac{dT}{dy}\alpha_{xy} \quad (26)$$

and in the same way

$$J_y = \sigma_{yy}E_y - \sigma_{yx}E_x + \frac{1}{T}\frac{dT}{dy}\alpha_{yy} - \frac{1}{T}\frac{dT}{dx}\alpha_{yx} \quad (27)$$

In the general case, the electrical and thermoelectric conductance in a transverse magnetic field are expressed in terms of the tensor components σ_{ij} and α_{ij} as in the equations (26) and (27).

The most important consequence of the assumptions asserted previously is that all elements of the conductivity tensor are expressed as weighted averages over the density of states ρ(ε), and zero field distribution, f(ε) in the coming derivations in accordance with

$$\langle \tau(\varepsilon) \rangle = \frac{\int_0^\infty \varepsilon\tau(\varepsilon)\left(\frac{\partial f_0}{\partial \varepsilon}\right)\rho d\varepsilon}{\int_0^\infty \varepsilon\left(\frac{\partial f_0}{\partial \varepsilon}\right)\rho d\varepsilon} \quad (28)$$

We use Onsager symmetry [20] for diagonal$\left(\sigma_{\parallel;}\, \alpha_{\parallel}\right)$ and off-diagonal$(\sigma_{\perp};\ \alpha_{\perp})$elements of electrical and thermoelectric conductivities to get

$$\sigma_{xx} = \sigma_{yy} = \frac{2e^2}{3m_n^*}\int_0^\infty \frac{\tau\varepsilon}{1+\omega^2\tau^2}\left(\frac{df_0}{d\varepsilon}\right)\rho d\varepsilon \quad (29)$$

$$\sigma_{xy} = -\sigma_{yx} = \frac{2e^2}{3m_n^*}\int_0^\infty \frac{\omega\varepsilon\tau^2}{1+\omega^2\tau^2}\left(\frac{df_0}{dE}\right)\rho d\varepsilon \quad (30)$$

$$\alpha_{xx} = \alpha_{yy} = \frac{2e}{3m_n^*}\int_0^\infty \frac{\tau\varepsilon}{1+\omega^2\tau^2}(\varepsilon - \varepsilon_F)\left(\frac{df_0}{dE}\right)\rho d\varepsilon \quad (31)$$

$$\alpha_{xy} = -\alpha_{yx} = \frac{2e}{3m_n^*}\int_0^\infty \frac{\omega\varepsilon\tau^2}{1+\omega^2\tau^2}(\varepsilon - \varepsilon_F)\left(\frac{df_0}{d\varepsilon}\right)\rho d\varepsilon \quad (32)$$

where for n-type semiconductor $df_0/d\varepsilon = -f_0/k_BT$.

Solving equations (26) and (27) for E_x and E_y gives

$$E_x = \frac{-J_x\sigma_{yy} + \frac{1}{T}\frac{dT}{dx}\sigma_{yy}\alpha_{xx} - \frac{1}{T}\frac{dT}{dy}\sigma_{yy}\alpha_{xy}}{-J_y\sigma_{xy} + \frac{1}{T}\frac{dT}{dy}\sigma_{xy}\alpha_{yy} - \frac{1}{T}\frac{dT}{dx}\sigma_{xy}\alpha_{yx}} \quad (33)$$

$$-\sigma_{xx}\sigma_{yy} + \sigma_{xy}\sigma_{yx}$$

and

$$E_y = \frac{-J_x\sigma_{yx} + \frac{1}{T}\frac{dT}{dx}\sigma_{yx}\alpha_{xx} - \frac{1}{T}\frac{dT}{dy}\sigma_{yx}\alpha_{xy}}{-J_y\sigma_{xx} + \frac{1}{T}\frac{dT}{dy}\sigma_{xx}\alpha_{yy} - \frac{1}{T}\frac{dT}{dx}\sigma_{xx}\alpha_{yx}} \quad (34)$$

$$-\sigma_{xx}\sigma_{yy} + \sigma_{xy}\sigma_{yx}$$

It can be written in vector form [19] as

$$\boldsymbol{E} = \boldsymbol{\rho J} + R_H(\boldsymbol{BXJ}) + S\boldsymbol{\nabla}T + N(\boldsymbol{BX}\nabla T) \quad (35)$$

where, we have electric resistivity (ρ), hall effect factor (R_H) that appears due to the application of the magnetic field that leads to a decrease in longitudinal conductivity and induces an off-diagonal conductivity, which is called the hall effect. This is commonly called the magneto-resistance. We have also Seebeck coefficient(S) and Nernst coefficient (N). When a conductive solid is placed under a longitudinal temperature gradient and a transverse magnetic field, two types of thermoelectric responses occur, i.e., the magneto-Seebeck effect in the longitudinal direction and the Nernst effect in the other transverse direction.

We can get magneto-Seebeck coefficient by setting $j_x = j_y = 0$ and eliminating E_y in equation (33) under isothermal condition $\nabla_y T = 0$ as

$$S = \frac{E_x'}{\nabla_x T} = -\frac{1}{T}\frac{\sigma_{yy}\alpha_{xx} + \sigma_{xy}\alpha_{yx}}{\sigma_{xx}\sigma_{yy} + \sigma_{xy}\sigma_{xy}}$$

$$= -\frac{1}{eT}\frac{\langle\frac{\tau}{1+\omega^2\tau^2}\rangle\langle\frac{\tau\varepsilon}{1+\omega^2\tau^2}\rangle + \langle\frac{\omega\tau^2}{1+\omega^2\tau^2}\rangle\langle\frac{\omega\tau^2\varepsilon}{1+\omega^2\tau^2}\rangle}{\langle\frac{\tau}{1+\omega^2\tau^2}\rangle^2 + \langle\frac{\omega\tau^2}{1+\omega^2\tau^2}\rangle^2} = -\frac{k_B}{e}\left\{\frac{K_0K_1 + \mu^2B^2\mathcal{L}_0\mathcal{L}_1}{K_0^2 + \mu^2B^2\mathcal{L}_0^2}\right\} \quad (36)$$

where the mobility $\mu = \frac{e\tau_0}{m_n^*}$ and the integral functions in equation (36) are expressed with the help of the reduced energy $x = \varepsilon/k_BT$ and $\tau = \tau_0 x^{3/2}$ accordingly other quantities which appeared in the derivations were reduced to dimensionless for sake of unit consistency.

$$K_i = \langle \frac{\tau\varepsilon^i}{1+\omega^2\tau^2} \rangle = \int_0^\infty \frac{x^{i+3} f_0}{1+\mu^2 B^2 x^3} dx \tag{37}$$

and

$$\mathcal{L}_i = \langle \frac{\omega\tau^2\varepsilon^i}{1+\omega^2\tau^2} \rangle = \int_0^\infty \frac{x^{i+9/2} f_0}{1+\mu^2 B^2 x^3} dx \tag{38}$$

Furthermore, Nernst coefficient is obtained by setting $j_x = j_y = 0$ and eliminating E_x in equation (33) under isothermal condition $\nabla_y T = 0$

$$N = \frac{E_y'}{\nabla_x T} = \frac{1}{T}\frac{\sigma_{xx}\alpha_{xy} - \sigma_{xy}\alpha_{xx}}{\sigma_{xx}\sigma_{yy} + \sigma_{xy}\sigma_{xy}}$$
$$= -\frac{k_B}{e}(\mu B)\frac{K_0\mathcal{L}_1 - K_1\mathcal{L}_0}{K_0^2 + \mu^2 B^2 \mathcal{L}_0^2} \tag{39}$$

We can obtain the corresponding expression for magneto-Seebeck coefficient for the case of modified density of states based on standard model with parabolic density of states (which doesn't incorporate the effect of band tails) by substituting equation (1) for modified density of states and by extending the integration limits from -∞ to ∞.

$$S = -\frac{k_B}{e}\left(\frac{\sqrt{2}\delta}{k_BT}\right)\frac{\psi_{5/2}'\psi_{7/2}' + c^2\psi_4'\psi_5'}{\psi_{5/2}'^2 + c^2\psi_4'^2} \tag{40}$$

where,

$$c = (\mu B)\left(\frac{\sqrt{2}\delta}{k_BT}\right)^{3/2} \tag{41}$$

and the integral functions in equation (40) are obtained by setting λ = 5/2; 7/2; 4; 5 into this equation respectively.

$$\psi_\lambda' = \frac{1}{2\pi^2}\int_{-\infty}^{0.601} \frac{|z\prime|^\lambda exp(-z\prime^2)(0.319 - 0.906 exp(2z\prime))}{exp\left(\frac{\sqrt{2}\delta}{k_BT}z\prime - \eta\right)\left(1 + \frac{e^2B^2\tau_0^2}{m_n^{*2}}\left(\frac{\sqrt{2}\delta}{k_BT}\right)^3 z\prime^3\right)} dz' + \int_{0.601}^{\infty} \frac{z\prime^{\lambda+1/2}\left[1 - \frac{1}{16z\prime^2}\right]}{exp\left(\frac{\sqrt{2}\delta}{k_BT}z\prime - \eta\right)\left(1 + \frac{e^2B^2\tau_0^2}{m_n^{*2}}\left(\frac{\sqrt{2}\delta}{k_BT}\right)^3 z\prime^3\right)} dz' \tag{42}$$

The corresponding expression for Nernst coefficient is

$$N = \frac{k_B}{e}\frac{\sqrt{2}\delta}{k_BT} c \frac{\psi_{5/2}'\psi_5' - \psi_4'\psi_{7/2}'}{\psi_{5/2}'^2 + c^2\psi_4'^2} \tag{43}$$

RESULTS

The calculation of Seebeck coefficient (S) for zero field used the expressions as $-\frac{k_B}{e}\frac{F_4}{F_3}$ and $-\frac{\sqrt{2}\delta}{eT}\frac{\psi_{7/2}}{\psi_{5/2}}$ for parabolic and non-parabolic bands respectively [21]. Similarly in the presence of magnetic field and temperature gradient equation (36) for Seebeck(S) and equation (39) for Nernst coefficient(N) in parabolic band and the corresponding equations equations (40) and (43) in non-parabolic are carried out under the assumption that the electron concentrations vary from $0.6 - 12\times10^{19}/cm^3$ and in the temperature range 77 – 300K. The effective mass of Mg_2Si is $m_n^* = 0.46m_0$(m_0 is mass of free electron) and its dielectric constant is $\epsilon = 20$ as well as the parameters $a_s$and δ were determined in the way as in [4].

Numerical values were obtained by using Matlab software in such a way that the reduced value of electron concentration $n_n = n/(10^{25}m^{-3})$ is used to get the corresponding reduced Fermi-energy η. A number of steps are required to get the write value of η for a given electron concentration through iterative method. Equation (11) for parabolic band was used and Equation (7) was for non-parabolic band in this iterative method in such a way that the integral on the LHS is evaluated for a given η and next one should get the write value which equates the given value of n_n on the RHS. That is how the calculated values were obtained. These values are the basis for the calculations of the thermomagnetic coefficients in the study in the presence of magnetic field varying in the range from 0.2 – 1T. Note that in this study electron mobility is taken to be featureless and the relaxation time is typically taken to be 10^{-11}s without losing the generality as in [19, 22,23].

Figure 1 is plotted with the calculated values of Seebeck coefficient for zero field case S(0) and S(B) in the presence of magnetic field that are used to determine Δ = S(B) –S(0) for parabolic and non-parabolic bands respectively. The change is significant for non-parabolic band consideration that is about 360μV/K on average compared to its value for parabolic band that is about 135.6 μV/k on average for magnetic field ranging in the interval 0.2 – 1T. In both cases there is enhancement of Seebeck coefficient due to magnetic field. As it is the case for this study, we need the modern approaches for better understanding of the thermomagnetic property of Mg_2Si–based materials based on the consideration

of non-parabolic band of heavily doped semiconductor rather than for that of parabolic band consideration. Due to this reason the value 360μV/K is reliable value that shows there is significant enhancement of Seebeck due to magnetic field for Mg_2Si–based materials. The enhancement of Seebeck coefficient 360 μV/K is two orders of magnitude greater than the experimental uncertainty level ~ 10 μV/K [24]. Therefore, one would expect significant effect of magnetic field in heavily doped n-type Mg_2Si.

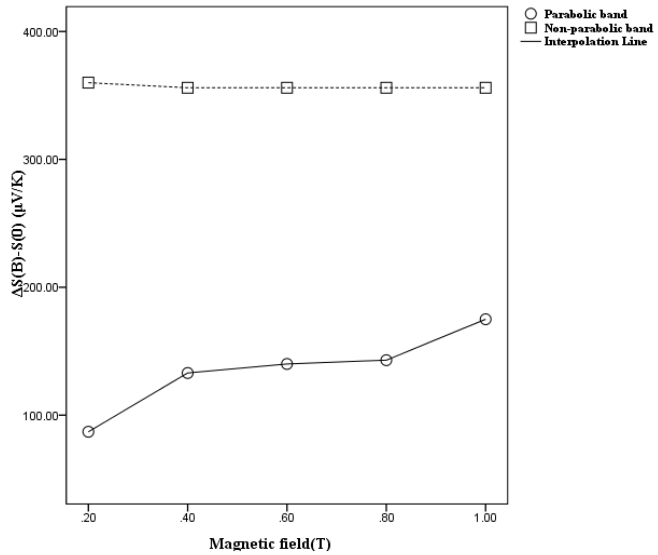

Figure 1. Change in Seebeck coefficient from non-zero field value S(0) to S(B) due to magnetic field for parabolic and non-parabolic bands

The result in Figure 2 provides the value of Nernst coefficient(N) as a function of magnetic field ranging in the interval 0.2 – 1T for electron concentration in heavily doping range 0.6 – $12\times10^{25}/m^3$ for parabolic band consideration. There is slow variation of Nernst coefficient with its negative values for certain electron concentrations such as $2\times10^{25}/m^3$ and $4\times10^{25}/m^3$ compared to relatively rapid variations for the rest values of electron concentrations. For the parabolic band consideration one can see the Nernst coefficient increases with magnetic field for the latter case.

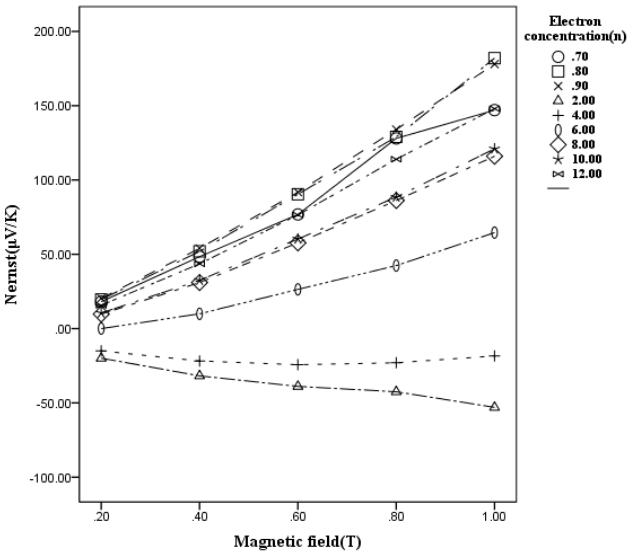

Figure 2. Nernst coefficient against magnetic field for different electron concentrations in parabolic band

The result in figure 3 is the value of Nernst coefficient as a function of magnetic field ranging in the interval 0.2 - 1T due to resolution problem in the graph it shows the average values for electron concentration in the heavily doping range 0.6 - $12\times10^{25}/m^3$. In contrast to the result in Figure 2 for parabolic band the Nernst coefficient decreases with magnetic field for non-parabolic band consideration with its magnitude in the order of 10^{-9} V/K compared to the order of magnitude 10^{-6} V/K for parabolic band consideration as shown in Figure 2. There is significant difference for order of magnitude of Nernst coefficient as a function of magnetic field for parabolic band consideration as compared to non-parabolic consideration. We are once again recommending using the more modern approaches in the consideration of non-parabolic band consideration as compared to parabolic consideration.

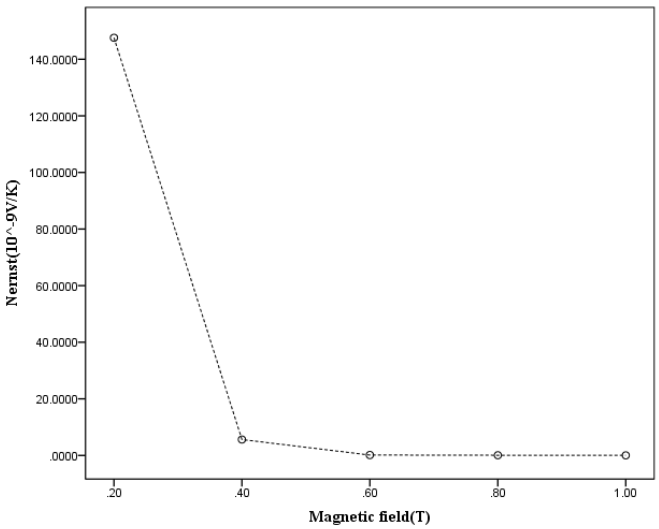

Figure 3. Nernst coefficient against magnetic field averaging its values for different electron concentrations in non-parabolic band

The same behavior as in figure 1 and figure 2 are expected to be observed for similar experimental arrangements. Therefore, there is a huge potential for further experimental explorations and investigations on such behaviors. These values are not meant to be good fits to measurements. Note that the results as shown are what we obtained with the help of Matlab software. Seebeck and Nernst coefficients should vary much with the magnetic field, so the results for these coefficients are closely agree with the first principle calculations as in [25] that show the importance of non-parabolic effects, in the thermoelectric properties of semiconductors. The same magneto Seebeck and Nernst behavior were experimentally observed according to experimental measurements [26] for polycrystalline Wely semimetal NbP.

CONCLUSION

Our theoretical calculation confirms that the material under study shows the general trend of exhibiting higher values of the magneto-Seebeck coefficients for non-parabolic band consideration compared to parabolic band consideration. Our theoretical results also show that the magnitude of the Nernst coefficient is larger at lower temperatures, lower carrier concentrations, and magnetic fields with the exception of that for non-parabolic consideration where Nernst coefficient shows decreasing trend with magnetic field. These observations could prove useful in evaluating the Nernst coefficient in other materials having similar band structures as that of Mg_2Si, while it is true that the relaxation times may differ with carrier concentration and magnetic field dependent mobility for our result to well agree with experimental result these factors should be considered in future studies for better result.

ORCID ID

Mulugeta Habte Gebru, https://orcid.org/0000-0001-7341-2717

REFERENCES

[1] P. Boulet, M.J. Verstraete, J.P. Crocombette, M. Briki, and M.C. Record, "Electronic properties of the Mg_2Si thermoelectric material investigated by linear-response density-functional theory," Computational Materials Science, **50**(3), 847-851 (2011). https://doi.org/10.1016/j.commatsci.2010.10.020

[2] N.S. Naser, R.V. Denys, H.F. Andersen, L. Arnberg, and V.A. Yartsy, "Nanostructured Magnesium silicide Mg_2Si and its electrochemical performance as anode of a Lithium battery," **718**, 478-491 (2017). https://doi.org/10.1016/j.jallcom.2017.05.163

[3] T.H. Nguyen, *et al.*, "On the composition of luminescence spectra from heavily doped p-type Silicon under low and high excitation," Journal of luminescence, **181**, 223-229 (2016). https://doi.org/10.1016/j.jlumin.2016.08.036

[4] M.H. Gebru, "Electrical and thermal conductivity of heavily doped n-type silicon," Eur. Phys. J. Appl. Phys. **90**, 10102 (2020). https://doi.org/10.1051/epjap/2020190332

[5] P.W. Chapman, O.N. Tufte, J.D. Zook, and D. Long, "Electrical properties of heavily doped silicon," J. App. Phys. **34**(11), 3291-3295 (2004). https://doi.org/10.1063/1.1729180

[6] W.G. Spitzer, F.A. Trumbore, and R.L. Logan, "Properties of heavily doped n-type germanium," Journal of Applied Physics, **32**, 1822–1830 (1961). https://doi.org/10.1063/1.1728243

[7] A. Cuevas, P.A. Basore, G.G. Matlakowski, and C. Dubois, "Surface Recombination Velocity of Heavily Doped N-Type Silicon," Journal of Applied Physics, **80**, 3370-3375 (1996). https://doi.org/10.1063/1.363250

[8] H. Zhou, P. Kropelnicki, J.M. Tsai, and C. Lee, "Study of the thermoelectric properties of heavily doped poly-Si in high temperature," Procedia Engineering, 94, 18-24 (2014). https://doi.org/10.1016/j.proeng.2013.10.011

[9] K. Kikuchi, K. Yamamoto, N. Nomura, and A. Kawasaki, "Synthesis of n-type Mg_2Si/CNT Thermoelectric Nanofibers," Nanoscale Res. Lett. **12**, 343 (2017). https://doi.org/10.1186/s11671-017-2120-y

[10] P. Kivinen, A. Savin, M. Zgirski, P. Törmä, J. Pekola, M. Prunnila, and J. Ahopelto, "Electro phonon heat transport and electrical conductivity in heavily doped silicon-on-insulator film," Journal of Applied Physics, **94**, 3201-3205 (2003). https://doi.org/10.1063/1.1592627

[11] G. Zhang, and B. Li, "Impacts of doping on thermal and thermoelectric properties of nanomaterials," Nanoscale, **2**, 1058-1068(2010). https://doi.org/10.1039/C0NR00095G
[12] D.W. Rowe, editor, *Thermoelectric Handbook: Macro to Nano*, (CRC Press/Taylor & Francis, Boca Raton, FL, 2006). https://doi.org/10.1201/9781420038903
[13] H. Wiggers, M.M. Schober, R. Koza, and P. Hermann, "Effects of impurity on the lattice dynamics of nanocrystalline silicon for thermoelectric application," J. Mater. Sci, **48**(7), 2836-2845 (2013). https://doi.org/10.1007/s10853-012-6827-y
[14] C.J. Hwang, "Calculation of Fermi energy and band tail parameters in heavily doped and degenerate n-type GaAs," J. Appl. Phys. **41**, 2268-2674 (1970). http://dx.doi.org/10.1063/1.1659280
[15] P.I. Baranskii, V.M. Babich, and E.F. Venger, "Development of The Physical Insight into The Nature of The Factors That Control Electrophysical and Other Properties of Semiconductors," Semiconductor Physics, Quantum Electronics & Optoelectronics, **4**(1), 1-4 (2000).4(2000). http://journal-spqeo.org.ua/users/pdf/n1_2001/001_4_1.pdf
[16] E.O. Kane, "Thomas-Fermi approach to impurity semiconductor band structure," Phys. Rev. **133**, 79-88 (1963). https://doi.org/10.1103/PhysRev.131.79
[17] C. Kittel, *Introduction to solid state physics*, 7th ed. (John Wiley & Sons Inc., New York, 1996).
[18] J.W. Slotboom, "The pn-product in silicon," Solid-State Electronics, **20**(4), 279-283 (1977). https://doi.org/10.1016/0038-1101(77)90108-3
[19] P. Sengupta, Y. Wen, and J. Shi, "Spin-dependent magneto-thermopower in narrow gaplead chalcogenide quantum wells," Sci. Rep. **8**, 5972 (2018). https://doi.org/10.1038/s41598-018-23511-2
[20] V. Zlatić, and R. Monnier, *The Modern Theory of Electricity*, (Oxford University press, 2014).
[21] M.H. Gebru, "Thermoelectric coefficients of heavily doped n-type silicon," East. Eur. J. Phys. **4**, 189-196 (2021). https://doi.org/10.26565/2312-4334-2021-4-25
[22] S.S. Lee, *Semiconducor physical electronics*, 2nded. (Springer, 2006).
[23] S.Majdi, N. Suntornwipat, M. Gabrysch, and J. Isberg,"Carrier scattering mechanisms: Identifications via the scaling properties of the Boltzmann transport equation," Advanced Theory and Simulations, **4**(1), 2000103 (2021). https://doi.org/10.1002/adts.202000103
[24] T.J. Salez, M. Kouyaté, C. Filomeno, M. Bonetti, M. Roger, G. Demouchy, E. Dubois, et al., "Magnetically enhancing Seebeck in ferrofluids," Nanoscale Adv. 1, 2979-2989 (2019). https://doi.org/10.1039/C9NA00109C
[25] X. Chen, D. Parker, and D.J. Singh, "Importance of non-parabolic band effects, on the thermoelectric properties of semiconductors," Sci. Rep. **3**, 3168 (2013). https://doi.org/10.1038/srep03168
[26] E.F. Scott, K.A. Schlaak, P. Chakraborty, C. Fu, S.N. Guin, S. Khodabakhsh, A.E.P. y Puente, et al., "Doping as Tuning Mechanism for Magneto-Thermoelectric Effects to Improveȥ T In Polycrystalline NbP," Phys. Rev. B, **107**, 115108 (2023), https://doi.org/10.1103/PhysRevB.107.115108

Appendix

Table 1. Calculated values for parabolic band model

Serial No	n_n	η	$\tau_{0,i}$	F_3	F_4	α_{xx} (μV/K)	B(T)	K_0	K_1	$\mathcal{L}_0$	$\mathcal{L}_1$	α_{xx} (μV/K)	N(μV/KT)
1	.6	-.26	1X10^-11s	4.62	18.5	-345		0.417	0.824	1.288	3.824	-244	-37.2
2	.7	-.11		5.38	21.5	-345		0.485	0.957	1.496	4.4428	-175.74	18.1
3	.8	.02		6.12	24.49	-348.9		0.552	1.09	1.704	5.06	-156	19.6
4	.9	.14		6.9	27.6	-34	0.2	0.622	1.229	1.921	5.705	-148.84	20.4
5	2	.94		15.36	61.4	-353.06		1.385	2.736	4.275	12.7	-194.199	-19.9
6	4	1.63		30.6	122.5	-345		2.762	5.454	8.523	25.31	-248.5	-15
7	6	2.04		46	184.6	-374.2		4.162	8.218	12.84	38.14	-285.2	-.1.05
8	8	2.3		59.85	239.4	-385.2		5.397	10.66	16.66	49.47	-313.9	9.75
9	10	2.55		76.8	307.4	-396		6.930	13.69	21.39	63.52	-338	10.5
10	12	2.73		92	367.98	-407.8		8.297	16.38	25.6	76.04	-359.2	15.7
1	.6	-.26						0.153	0.2566	0.379	1.04	-102	14200
2	.7	-.11						0.177	0.298	0.44	1.209	-107.5	48.4
3	.8	.02						0.202	0.34	0.501	1.377	-112.7	52
4	.9	.14						0.228	0.383	0.565	1.55	-117.3	54.0
5	2	.94					0.4	0.506	0.85	1.257	3.456	-162.5	-31.8
6	4	1.63						1.01	1.7	2.51	6.89	-215.6	-21.8
7	6	2.04						1.521	2.56	3.78	10.38	-253.9	9.94
8	8	2.3						1.973	3.32	4.9	13.46	-284.9	31
9	10	2.55						2.53	4.26	6.29	17.29	-311.4	32.5
10	12	2.73						3.03	5.102	7.53	20.7	-334.7	43.6
1	.6	-.26						0.08	0.124	0.178	0.474	-95.7	130000
2	.7	-.11						0.09	0.144	0.207	0.551	-101.7	76.8
3	.8	.02						0.106	0.164	0.235	0.627	-107.3	90.4
4	.9	.14						0.119	0.185	0.265	0.707	-112.4	91.8
5	2	.94					0.6	0.266	0.41	0.59	1.57	-156.3	-38.9
6	4	1.63						0.529	0.819	1.177	3.14	-208.2	-24.3
7	6	2.04						0.798	1.23	1.77	4.73	-246	26.4
8	8	2.3						1.035	1.601	2.3	6.13	-276.8	57.7
9	10	2.55						1.33	2.056	2.95	7.87	-303.2	60.3
10	12	2.73						1.59	2.46	3.54	9.43	-326.6	76.5
1	.6	-.26					0.8	0.05	0.073	0.103	0.27	-93.7	14100
2	.7	-.11						0.058	0.084	0.119	0.31	-99.6	128

Serial No	n_n	η	$\tau_{0,i}$	F_3	F_4	α_{xx} (μV/K)	B(T)	K_0	K_1	$\mathcal{L}_0$	$\mathcal{L}_1$	α_{xx} (μV/K)	N(μV/KT)
3	.8	.02						0.066	0.096	0.136	0.36	-105.2	129
4	.9	.14						0.074	0.11	0.1534	0.402	-110.3	134
5	2	.94						0.165	0.24	0.34	0.895	-153.7	-42.5
6	4	1.63						0.328	0.48	0.68	1.78	-204.9	-23
7	6	2.04						0.495	0.725	1.025	2.69	-242.4	42.4
8	8	2.3						0.64	0.94	1.33	3.49	-272.93	86.2
9	10	2.55						0.82	1.207	1.71	4.476	-299.21	88.5
10	12	2.73						0.986	1.445	2.04	5.36	-322.5	114
1	.6	-.26						0.034	0.048	0.067	0.17	-92.5	15600
2	.7	-.11						0.039	0.056	0.078	0.2	-98.5	147
3	.8	.02						0.045	0.06	0.089	0.23	-104	182
4	.9	.14						0.05	0.07	0.1	0.259	-109.2	178
5	2	.94						0.11	0.159	0.22	0.58	152.2	-53
6	4	1.63					1	0.224	0.316	0.44	1.15	-203	-18.4
7	6	2.04						0.34	0.476	0.667	1.73	-240.3	64.6
8	8	2.3						0.438	0.62	0.865	2.24	-270.7	116
9	10	2.55						0.56	0.79	1.11	2.88	-296.9	121
10	12	2.73						0.67	0.95	1.33	3.45	-320	148

Table 2. Calculated values for non-parabolic band model

Serial No	n_n	η	$\tau_{0,}$	$\Psi_{5/2}$	$\Psi_{7/2}$	α_{xx} (μV/K)	B(T)	Ψ'_4	Ψ'_5	$\Psi'_{5/2}$	$\Psi'_{7/2}$	α_{xx} (μV/K)	N(μV/K)
1	.6	-.15	1X10^-11s	4.21	16.53	-334	0.2T	1.136	3.25	0.372	0.733	-243.6	26.9
2	.7	.029		3.99	14.87	-332		0.886	2.53	0.287	0.57	-175.7	8.8
3	.8	.22		13.14	13.15	-342.8		0.78	2.11	0.275	0.52	-156	4.97
4	.9	.4		3.63	12.18	-329.2		0.208	0.338	0.26	0.48	-148.8	-.28
5	2	1.57		3.19	7.07	-345.6		0.175	0.34	0.097	0.136	-194.2	.79
6	4	3.1		3	6.37	-332		0.166	0.292	0.094	0.13	-248.5	.23
7	6	4.28		3.46	6.89	-368.6		0.129	0.214	0.082	0.106	-285.2	.17
8	8	5.8		5.33	10.9	-379.8		0.13	0.228	0.075	0.104	-314	.16
9	10	6.8		6.14	12.57	-390.9		0.11	0.2	0.062	0.089	-338	.118
10	12	7.08		5.2	10.15	-402.2		0.082	0.14	0.048	0.066	-359.2	0.06
1	.6	-.15					0.4T	0.676	1.99	0.22	0.436	-102	1.8
2	.7	.029						0.26	0.685	0.098	0.173	-107.5	0.3
3	.8	.22						0.257	0.59	0.157	0.197	-112.6	0.6
4	.9	.4						0.197	0.49	0.083	0.138	-117.3	0.17
5	2	1.57						0.08	0.155	0.0455	0.0625	-162.5	0.004
6	4	3.1						0.044	0.076	0.027	0.0361	-215.6	0.001
7	6	4.28						0.033	0.055	0.02	0.027	-253.9	0.0007
8	8	5.8						0.0334	0.058	0.02	0.027	-284.9	0.001
9	10	6.8						0.0287	0.051	0.016	0.0227	-311.4	0.0007
10	12	7.08						0.021	0.035	0.013	0.017	334.7	0.0004
1	.6	-.15					0.6T	0.144	0.398	0.056	0.097	-95.7	0.008
2	.7	.029						0.118	0.309	0.047	0.081	-101.7	0.005
3	.8	.22						0.1007	0.256	0.039	0.069	-107.3	0.003
4	.9	.4						0.09	0.22	0.042	0.065	-112.4	0.003
5	2	1.57						0.036	0.07	0.02	0.029	-156.3	0.0006
6	4	3.1						0.02	0.034	0.0123	0.016	-208.2	0.0003
7	6	4.28						0.015	0.024	0.009	0.012	-246	0.0001
8	8	5.8						0.015	0.026	0.008	0.012	-276.8	0.0001
9	10	6.8						0.013	0.023	0.007	0.01	-303.2	0.0001
10	12	7.08						0.009	0.016	0.006	0.0075	-326.6	0.0001
1	.6	-.15					0.8T	0.676	1.99	0.22	0.436	-93.7	1.27
2	.7	.029						0.047	0.176	0.0218	0.044	-99.6	0.002
3	.8	.22						0.058	0.145	0.026	0.04	-105.2	0.002
4	.9	.4						0.051	0.124	0.02	0.036	-110.3	0.0007
5	2	1.57						0.02	0.039	0.013	0.016	-153.7	0.0003
6	4	3.1						0.01	0.019	0.007	0.009	-204.9	0.0001
7	6	4.28						0.011	0.019	0.0074	0.0094	-242.4	0.0001
8	8	5.8						0.008	0.015	0.005	0.007	-272.9	0.00007
9	10	6.8						0.007	0.013	0.004	0.006	-299.2	0.00004
10	12	7.08						0.005	0.009	0.003	0.004	-322.5	0.00003
1	.6	-.15					1T	0.054	0.145	0.04	0.038	-92.5	0.000000
2	.7	.029						0.044	0.11	0.02	0.03	-98.5	0.0008
3	.8	.22						0.038	0.094	0.0158	0.0263	-104	0.0005
4	.9	.4						0.034	0.08	0.0166	0.0244	-109.2	0.0005
5	2	1.57						0.013	0.025	0.008	0.01	-152.2	0.0001
6	4	3.1						0.007	0.012	0.0036	0.0057	-203	0.000008
7	6	4.28						0.005	0.009	0.003	0.004	-240.3	0.00002
8	8	5.8						0.0054	0.0093	0.003	0.0043	-270.7	0.000017
9	10	6.8						0.0046	0.008	0.003	0.0036	-296.9	0.00003
10	12	7.08						0.003	0.0056	0.002	0.0027	-320	0.00001

МАГНІТО-ТЕРМОЕЛЕКТРИЧНІ КОЕФІЦІЄНТИ СИЛЬНОЛЕГОВАНОГО МАТЕРІАЛУ N-ТИПУ Mg2Si

Мулугета Хабте Гебру

Факультет фізики, Університет Арба Мінча, Арба Мінч, Ефіопія

На відміну від параболічної смугової моделі, яка зазвичай використовується для розуміння електронних властивостей загалом, термоелектричних і магнітотермоелектричних зокрема, це дослідження підтверджує результати непараболічної смугової моделі для кращого розуміння коефіцієнтів Зеєбека та Нернста в присутності магнітного поля для Mg_2Si. Коефіцієнт магнето Зеєбека був значно підвищений порівняно з ненульовим значенням поля як функція магнітного поля для різних концентрацій електронів у діапазоні $0.6\text{-}12\times10^{25}/m^3$ в середньому при кімнатній температурі для непараболічної моделі порівняно з параболічною. модель гурту. Результат для коефіцієнта Нернста демонструє тенденцію до зростання як функції магнітного поля, за винятком певних концентрацій електронів для моделі параболічної зони. Водночас вона зменшується з магнітним полем у середньому для моделі непараболічної зони.

Ключові слова: *коефіцієнт магнето-Зеєбека; коефіцієнт Нернста; сильнолегований напівпровідник; магнітотермоелектрика; силіцид магнію*